Structure of Human Telomeric DNA G-Quadruplexes in a Model Cell-Like Confined Environment Using a Fluorescent Nucleoside Probe

A thesis submitted towards partial fulfillment of the requirements of

BS-MS Dual Degree Program

By

SARANGAMATH SANGAMESH

20101036

Indian Institute of Science Education and Research Pune

Under the guidance of

Dr. S. G. SRIVATSAN

Associate Professor

Department of Chemistry

Indian Institute of Science Education and Research Pune

Certificate

This is to certify that this dissertation entitled "Structure of Human Telomeric DNA G-Quadruplexes in a Model Cell-Like Confined Environment Using a Fluorescent Nucleoside Probe" towards the partial fulfillment of the BS-MS dual degree programme at the Indian Institute of Science Education and Research, Pune represents original research carried out by Sarangamath Sangamesh at IISER Pune under the supervision of Dr. S. G. Srivatsan, Associate Professor, Department of Chemistry, IISER Pune during the academic year 2014-2015.

Date: 25/03/2015
Place: Pune

S. G. Srivatsan

Dr. S. G. Srivatsan
Associate Professor
Department of Chemistry
IISER Pune

डॉ. एस. जी. श्रीवत्सन/ Dr. S. G. Srivatsa
सहभागी प्रशासक, रसायनशास्त्र/ Associate Professor, Chemistry
भारतीय विज्ञान शिक्षा एवं अनुसंधान संस्थान
Indian Institute of Science Education & Research
पुणे-411 008, भारत/ Pune - 411 008, India

Declaration

I hereby declare that the matter embodied in the report entitled "**Structure of Human Telomeric DNA G-Quadruplexes in a Model Cell-Like Confined Environment Using a Fluorescent Nucleoside Probe**" are the results of the investigations carried out by me at the Department of Chemistry, Indian Institute of Science Education and Research, Pune, under the supervision of Dr. S. G. Srivatsan and the same has not been submitted elsewhere for any other degree.

Date: 25th March 2015

Place: Pune

**Sarangamath
Sangamesh**

<u>Acknowledgements</u>

Dedicated to my parents and Bhadra

Table of contents

List of figures

List of tables

Abstract

Nucleic acids play a central role in carrying genetic information, and also have the ability to catalyze biochemical reactions and regulate gene expression in the cell. Their functions often involve conformational changes while interacting with other nucleic acids, proteins and small molecule metabolites. Several biophysical tools have been developed which report these conformation changes *in vitro*. In particular, microenvironment-sensitive fluorescent nucleoside analogues have afforded effective biophysical tools to understand the structure, dynamics and function of nucleic acids. However, their use has been limited to *in vitro* studies because of low quantum yield when incorporated into oligonucleotides and or their excitation maximum in the UV region. Self-assembling systems like reverse micelles, which are UV transparent, have been reported to have the similar physical properties in their aqueous core as observed in the cellular environment and provide necessary macromolecular crowding effects, thus making them as useful cell mimicking systems.

In this context, here we report the photophysical studies of environment-sensitive fluorescent nucleoside analogue, 5-(benzofuran-2-yl)-2'-deoxyuridine (BFdU), in micellar and reverse micellar systems. The nucleoside analogue senses the change in the microenvironment of micelles and in the core of reverse micelles. Furthermore, we have used the environment-sensitivity of nucleoside in studying the structure of human telomeric DNA sequence in reverse micelles, which served as a model cell-like confined environment. Steady-state fluorescence and lifetime studies suggest that the nucleoside analogue incorporated into telomeric DNA repeat successfully senses the changes in the metal ion dependent conformational changes in buffer systems and in AOT reverse micellar systems. Also it can photo physically distinguish between G-quadruplexes and corresponding duplexes in AOT reverse micelles. Hence it can be used as a non-invasive robust tool for the detection and conformational studies of G-quadruplex structures.

1. Introduction

Nucleic acids play a very important role by carrying the genetic material and passing on them to the next generation. All the genetic material is stored in the form of a variety of combinations of just four molecules: Adenine (A), Guanine (G), Thymine (T) and Cytidine (C). Nucleic acids apart from carrying the genetic information are also involved in a lot of other crucial functions by catalyzing the biochemical reactions. They carry out their functions by interacting with other nucleic acids, proteins and other molecules. One of the important ways by which these functions are carried out is by changes in their conformations. One of the classes of secondary nucleic acid structures which are being studied extensively are G-quadruplexes.[1] Various biophysical techniques such as NMR, EPR, fluorescence, X-ray crystallography and UV-visible spectroscopy have been utilized to study these conformational changes.[2–4] The most widely used technique is fluorescence spectroscopy owing to its very high sensitivity, ease of experimentation and the ability to get the information in real time. In particular, fluorescent nucleoside analogues have gained a lot of attention recently because of their sensitivity to the surrounding microenvironment, and their ability to minimally perturb the native structures of nucleic acids (Figure 1).[5–8]
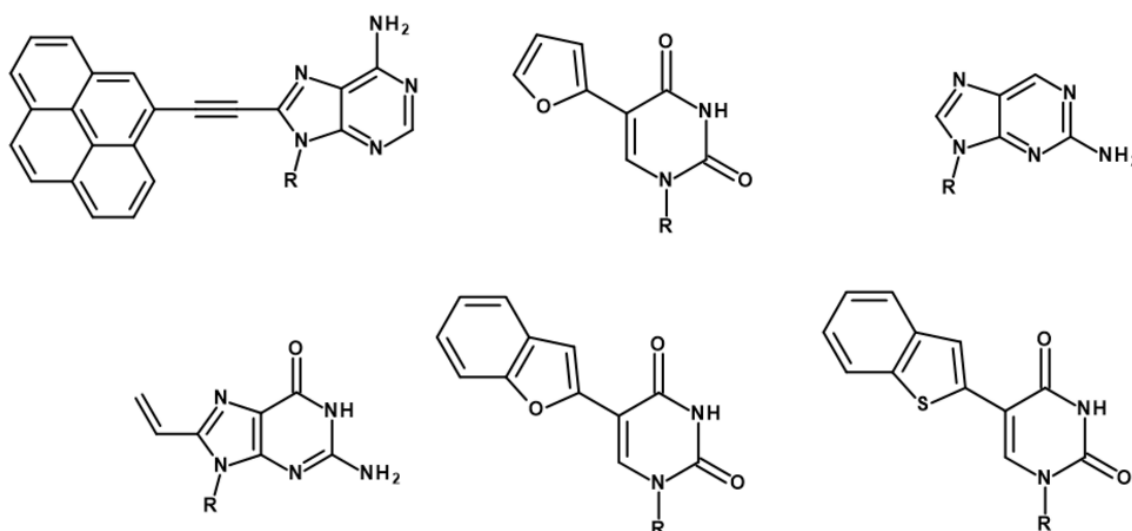
Figure 1. Environment-sensitive fluorescent nucleoside analogues.

1.1. G-quadruplexes

Nucleic acids are generally assumed to have a double stranded helix structure. But even before the double stranded helix structure was elucidated it had been observed that guanine bases in solution undergo self-association and form a planar quartet structure where the four guanine molecules are bonded to each other by Hoogsteen hydrogen bonding interactions.[9] Recently, in the last twenty years there have been a lot of reports showing that the guanine rich nucleic acid stretches in the genome can form such tetrads. These have been called as G-quadruplexes.[10,11] These are non- canonical secondary nucleic acid structures. As described earlier, the four guanines are bonded to each other by Hoogsteen hydrogen bonding interactions. This is a planar arrangement. At the center of the tetrad, there are four oxygen atoms which need to be stabilized. This happens by metal ions like K^+ and Na^+. This makes them a very good metal binding ligands (Figure 2).[12]
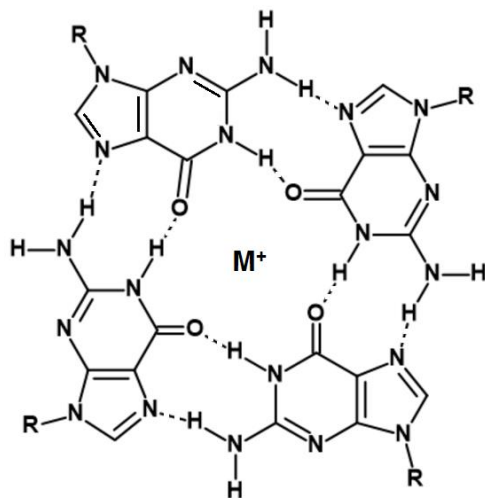
Figure 2. Structure of G-quartet. R = Sugar-phosphate groups. M^+ = stabilizing metal ions.

There can be a wide variety of conformations these G-rich sequences can form (Figure 3). G-quadruplexes can be formed by intra-strand folding where repeated stretches of guanines in a single oligonucleotide sequence stack together to form G-tetrads or two or more oligonucleotide sequences rich in guanine bases can stack up to form G-tetrads. These are called inter-strand G-quadruplexes. These G-quadruplex structures can fold into parallel, anti-parallel or mixed hybrid structures depending on the solution conditions, hydration effects, molecular crowding effects by the co solutes,

and the stabilizing metal ions.[13–15] They are known to form antiparallel conformations in the presence of Na$^+$ ions, hybrid structures in the presence of K$^+$ ions and extensive parallel conformations in the presence of K$^+$ ions in molecular crowding medium like polyethylene glycol.[12,15–18] This directionality is assigned by the directions of the strands (5' to 3'). The quadruplex structure with all the four strands participating in the tetrad having same directionality i.e. 5' to 3' is assigned as parallel quadruplex. The quadruplex with strands where the alternate or the opposite strands go in the opposite directions i.e. one in 3' to 5' and the other in 5' to 3', is termed as antiparallel G-quadruplex structure. A third conformation is possible where there are both parallel and antiparallel directionalities. This conformation is termed as hybrid structure.[12]

a. Antiparallel quadruplex.

b. Parallel quadruplex

c. Hybrid quadruplex
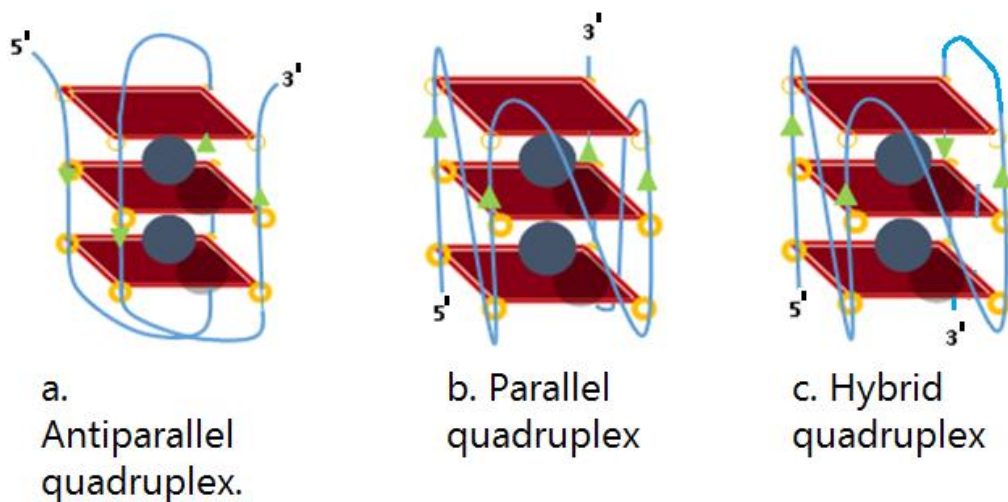
Figure 3. Structures of various forms of G-quadruplexes. a. Antiparallel in Na$^+$, b. Parallel in molecular crowding agent/K$^+$ crystal structure, c. Hybrid structure in aqueous solutions containing K$^+$. The arrows denote the directionality. Blue spheres represent stabilizing metal ions.

Recently, it has been shown by Shankar Balasubramanian's group that these G-quadruplex structures are indeed present in human cells at physiological conditions using antibody, which is specific to G-quadruplexes.[19,20] Also, they have shown that G-quadruplexes are formed during the (synthesis) S1 phase of the cell cycle where DNA gets replicated. They have also shown that pyridostatin a small molecule ligand binds specifically to these quadruplexes and stabilizes the GQ conformations.[19,20]

G-quadruplex structures have been found in telomeres and at the transcription promoter regions and are involved in key biological processes like maintenance of

chromosome integrity, in gene regulation and gene silencing.[21,22] These structures are directly involved in tumours thus, making them a potential target for cancer therapy.[23–25] Studying their structure and dynamics is of great importance. A lot of research has happened in this area where researchers have found out their direct involvement in tumours and for probing these structures tools like antibody labelling, click chemistry and extrinsic fluorescent dyes have been used.[12,26,27] Fluorescent nucleoside analogues, among all the other biophysical tools, have been widely used because of their non-invasive nature and their sensitivity towards the surrounding microenvironment. But, very few reports are present where the G-quadruplex structures have been studied by incorporating fluorescent nucleoside analogues.[28–30] Thus it is crucial for the development of probes which are minimally perturbing, have their excitation maxima in the visible region and high quantum yields so that they can be used in cell based assays, and will allow us to elucidate these conformational dynamics *in vivo*.

1.2. Micelles

Surfactants are a class of amphiphiles which consist of one or more long hydrophobic alkyl chains and a hydrophilic head group. When added in a polar solvent, these molecules change the surface properties of the solvent drastically (e.g. reduction in the surface tension). But as their concentration is increased, they start self-assembling into macromolecules called micelles (Figure 4). This occurs at a particular concentration called as critical micellar concentration (CMC). When a surfactant is added into a polar solvent like water, these molecules start self-assembling into various structures, after the CMC, where the hydrophilic head groups are oriented to the outside and the inner core consists of hydrophobic alkyl chains. This self-assembly happens in order to minimize the energy of the whole surfactant-solvent system so that the system is thermodynamically stable. These micellar structures are dynamic in nature. There is a drastic change in the properties like conductivity, surface tension, polarity and viscosity below and above the CMC. People have used different techniques like UV, fluorescence spectroscopy, conductivity methods, and surface tension methods to study these changes.[31–33]
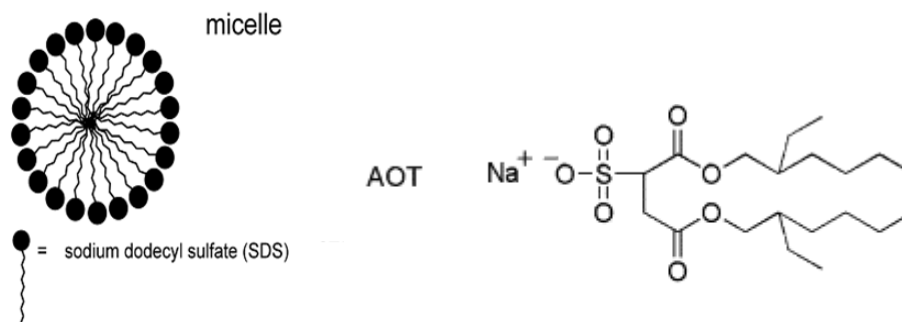
Figure 4. Diagrammatic representation of a micelle[34] and dioctyl sodium sulphosuccinate (AOT).

1.3. Reverse Micelles

AOT surfactant molecules, when dissolved in a non-polar solvent like n-heptane self-assemble into reverse micellar structures where the hydrophobic alkyl chain faces n-heptane. The inner core consists of the hydrophilic part. But when water is added to this system the reverse micelles encapsulate the water molecules in the inner hydrophilic core and the structure becomes spherical.[35,36] The encapsulated water has very different properties than the bulk water.[37] The pH inside the AOT reverse micelles is generally basic when the counter ion is sodium. The water molecules inside the reverse micelles have significantly reduced motion and the medium is viscous.[10,38,39] The size of the encapsulated nanosized water core increases with the increase in the addition of water. The size of the reverse micelles is generally quantified by the W_0 value which is the molar ratio of water to surfactant.[40] This has been determined by X-ray and neutron scattering.[41–43] Also the radius of the reverse micelle is directly proportional to the W_0 value.[40] At very low W_0 values most of the water molecules interact with the ionic head groups of the AOT surfactants. When the W_0 is increased above 6 a definite water pool starts forming. The properties of this water pool are very different from that of the interfacial water molecules. The viscosity is lower in this pool and the water molecules have higher mobility and are more polar. In general the viscosity decreases with increases in W_0 value.[38] Also the polarity increases with the increase in W_0 value.[44]

6

1.4. Aim

G-quadruplexes play a crucial role in important biological processes. They are a promising candidates as the targets for cancer therapy and anti-aging.[21,22,24] Thus, fundamental understanding about the structure, and conformational dynamics of these structures is necessary. This motivated the incorporation of an environment-sensitive fluorescent nucleoside analogue BFdU,[45] into a biologically important, G-quadruplex forming oligonucleotide, human telomeric sequence(HTS), and use it as a probe to study the metal ion dependent conformational dynamics. Since, BFdU cannot be used in *in vivo* studies because of its excitation maximum in UV region, a well-known, UV transparent, cell mimicking system, dioctyl sodium sulphosuccinate (AOT) reverse micelle has been used as a cell model. AOT reverse micellar inner aqueous core provide the necessary molecular crowding effects which are present in cellular systems.[46]

2. Experimental Section

2.1. Materials

Sodium dodecyl sulphate (SDS) was obtained for SRL India Limited. n-heptane (HPLC grade) was obtained from RANKEM India. Dioctyl sodium sulfosuccinate (AOT), 5-Iodouracil, 2-benzofuran, bis(triphenylphosphine)-palladium (II) chloride, were obtained from Sigma-Aldrich. AOT was dried under vacuum for 48 h before use. Benzofuran modified oligonucleotide (BFGQ) was synthesized by solid phase synthesis by one of my colleagues, Arun Tanpure. Autoclaved water was used in all spectroscopic experiments.

2.2. Fluorescence properties of BFdU in micelles

Steady state fluorescence experiments: A series of aqueous solutions, containing different concentrations of the surfactant SDS in water were prepared. A fixed amount of BFdU (25 µL) was added to each of the solutions so that the final concentration of the fluorophore is maintained at 5 µM and the samples were sonicated for one minute. The solutions were kept in dark for 3 hours, to equilibrate, before taking the fluorescence readings. The solutions were excited at 322 nm. The excitation and emission slit widths were kept at 2 and 3 nm, respectively. The measurements were taken in Horiba Fluoromax-4 spectrofluorometer. A blank in the absence of fluorophore was taken and was subtracted from each sample. These experiments were performed in triplicate at 25 °C in a quartz microcuvette. To estimate the CMC of SDS, plot of fluorescence intensity at emission maximum versus concentration of SDS was fitted with a non-linear sigmoidal curve fitting using Boltzmann function (Origin software). The formula used was:

$$y = \frac{A_1 - A_2}{1 + e^{\left(\frac{x - x_0}{\Delta x}\right)}} + A_2$$

Where y = fluorescence intensity at 448 nm, x is the concentration of the surfactant (here [SDS]), x_0 is the centre of sigmoid which gives the CMC of the surfactant, **Δx** = slope factor, A_1 = upper limit of fluorescence intensity, A_2 = fluorescence intensity in the absence of surfactant.

Steady-State Anisotropy measurements: The fluorescence anisotropy experiments were carried out at three different conditions, one below the CMC value of SDS (where there are no micelles) i.e. at 2 mM, one around CMC value (where the micelles start forming) i.e. at 10 mM and one above CMC value (where the majority of the molecules are in micellar state) i.e. at 20 mM. The experiments were carried out in Fluoromax-4 spectrofluorometer (Horiba JobinYvon). The samples were excited at 322 nm and at the respective emission maxima, their emission intensities were collected. Each anisotropy value is an average of 10 consecutive measurements for each sample. Measurements were performed in triplicate at 25 $^\circ$C. The anisotropy and polarization values were directly calculated and given by the software provided with the instrument.

Time resolved fluorescence measurements: To determine the excited-state decay kinetics of the fluorescent nucleoside analogue in the presence and absence of micelles a series of different concentrations of SDS in water were prepared. In each sample a fixed amount of BFdU (5 μM) with 0.5% DMSO was added. The samples were allowed to equilibrate for 2 hours before the measurements were taken. The samples were excited with a diode laser of 339 nm (IBH, UK, NanoLED-339L) at 25 $^\circ$C. The decay profiles were collected at the respective emission maxima and were analyzed using the software, IBH DAS6. The effect of scattering was taken care of by using LUDOX prompt. For all the decay profiles the value of χ^2 were close to unity.

2.3. Fluorescence properties of BFU in AOT RM

Stock solutions of AOT were prepared in HPLC grade n-heptane. Appropriate amount from Stock solutions of BFU in water (with <5% DMSO) were added to the glass vials containing AOT reverse micelles so that the resultant solutions contain corresponding W_0 values and the final concentration of BFU and AOT in each sample is maintained at 1 μM and 200 mM, respectively. The samples were sonicated for 30 seconds and were kept in dark for nearly two hours to attain equilibrium before the fluorescence anisotropy experiments were conducted. After adding the stock solution of the nucleoside analogue to AOT RM the solution becomes hazy and only after sonication, the solution becomes

clear again implying that the water molecules are encapsulated inside the reverse micellar core of AOT.

Steady state fluorescence measurements: For the steady state experiments the samples were excited at 322 nm. The excitation and emission slit widths were kept at 3 and 4 nm, respectively. For each of the sample a spectral blank in the absence of the fluorophore at the corresponding W_0 value was subtracted. The experiments were conducted at 25 $^\circ$C in triplicate in a quartz micro fluorescence cuvette.

Time resolved fluorescence measurements: Each of the samples with different W_0 values containing 1 µM of BFU and 200 mM AOT were prepared in glass vials. All the samples were sonicated for 20 seconds and were kept in dark for nearly 2 hours before measuring the excited state decay kinetics. The samples were excited with a 339 nm diode laser (IBH, UK, NanoLED-339L) at 25 $^\circ$C. The decay profiles were collected at the respective emission maxima and were analyzed using the software, IBH DAS6. The effect of scattering was taken care of by using LUDOX prompt. For all the decay profiles the value of χ^2 was close to unity.

2.4. Purification of BFGQ oligonucleotide by Gel Electrophoresis

The deprotected oligonucleotide sequence (BFGQ), which was synthesized by Arun Tanpure was purified by 20% polyacrylamide gel electrophoresis under denaturing conditions. The sequences were visualized by UV shadowing and the product bands were removed from the gel and transferred to a Bio-Rad poly-prep column. The pieces of gel were crushed using a sterile glass rod. Extraction was done in sodium acetate buffer for 12 hours. The resulting solutions were filtered and desalted in Sep-Pak classic C18 cartridges (Waters).

2.5. Fluorescence properties of BFGQ in AOT reverse Micelles

BFGQ in AOT-sodium salt: 100 µM of BFGQ in water was prepared by dilution from the main stock of 723 µM. Stock solutions of BFGQ (53 µM) in Tris buffer (10 mM, pH 7.5) containing 50 mM of NaCl or KCl were prepared by annealing at 90 $^\circ$C for 3 min and then

allowing them to come to room temperature slowly. Later the samples were put in crushed ice for 2 hours. From the hybridised stock (53 µM), 37 µL was added to 450 µL of AOT in n-heptane to make the final concentration of BFGQ, W_0 value, and the concentraion of AOT to be 4 µM, 20 and 0.2 M, respectively. The samples were centrifuged for 10 seconds, sonicated for 5 seconds and kept for 3 hours to equilibrate before taking the measurements. There was an issue of solubility with concentrations higher than 50 mM for both the salts. So, they have not been done.

BFGQ duplex in AOT-sodium salt: 200 µM of CGQ (complementary strand of BFGQ) in water was prepared from the main stock of 670 µM. 723 µM BFGQ was directly used without further dilution. Stock solutions of BFGQ:CGQ (53 µM) in Tris buffer (10 mM, pH 7.5) containing 50 mM of NaCl or KCl were prepared by annealing 1:1 mixture of both the oligonucleotides at 90 °C for 3 min and then allowing them to come to room temperature slowly. Later the samples were put in crushed ice for 2 hours. From the hybridised stock (53 µM), 37 µL was added to 450 µL of AOT in n-heptane to make the final concentration of BFGQ, W_0 value, and the concentraion of AOT to be 4 µM, 20 and 0.2 M, respectively. The samples were centrifuged for 10 seconds, sonicated for 5 seconds and kept for 3 hours before taking the measurements.

Steady-state fluorescence measurements: Steady-state fluorescence measurements were taken in Fluorlog-3 Horiba Yvon, Fluoromax-4 spectrofluorometer at 25 °C. The samples were excited at 322 nm by keeping the excitation and emission slit widths at 2 and 4 nm, respectively. All the measurements are taken in replica and are subtracted from the respective blanks containing buffer solutions or AOT reverse micelles with W_0 = 20 in the absence of the oligonucleotides.

Time-resolved fluorescence measurements: The samples were excited using a 339 nm diode laser (IBH, UK, NanoLED-339L) at 25 °C. Emission signals at the respective emission maxima were collected. The experiments were done in replica. The decay profiles were analyzed using IBH DAS6 software provided by the instrument. The curve fitting for all the samples has been done by taking the scattering effects into consideration. For this LUDOX has been used as the prompt. For all the decay profiles the value of χ^2 were close to unity.

3. Results and Discussion

3.1. Synthesis of fluorescent nucleoside analogues

Both 5-(benzofuran-2-yl)-2'-deoxyuridine (BFdU) and 5-(benzofuran-2-yl)uridine (BFU) were synthesized by following the procedure reported by Tanpure et al.[45,47] Stille cross coupling reaction conditions were used wherein 2-(tri-butylstannyl)benzofuran was reacted with 5-iodo-uridine or 5-iodo-2'-deoxyuridine. These reactions were performed in the presence of a palladium catalyst, $Pd(PPh_3)_2Cl_2$ for 3 hours. Here Pd^0 is the active catalyst. Dark coloration of the reaction mixture confirms the successful reduction of palladium to Pd^0 and also an indication that the reaction mixture is devoid of moisture since these reactions are sensitive to moisture (Scheme 1).
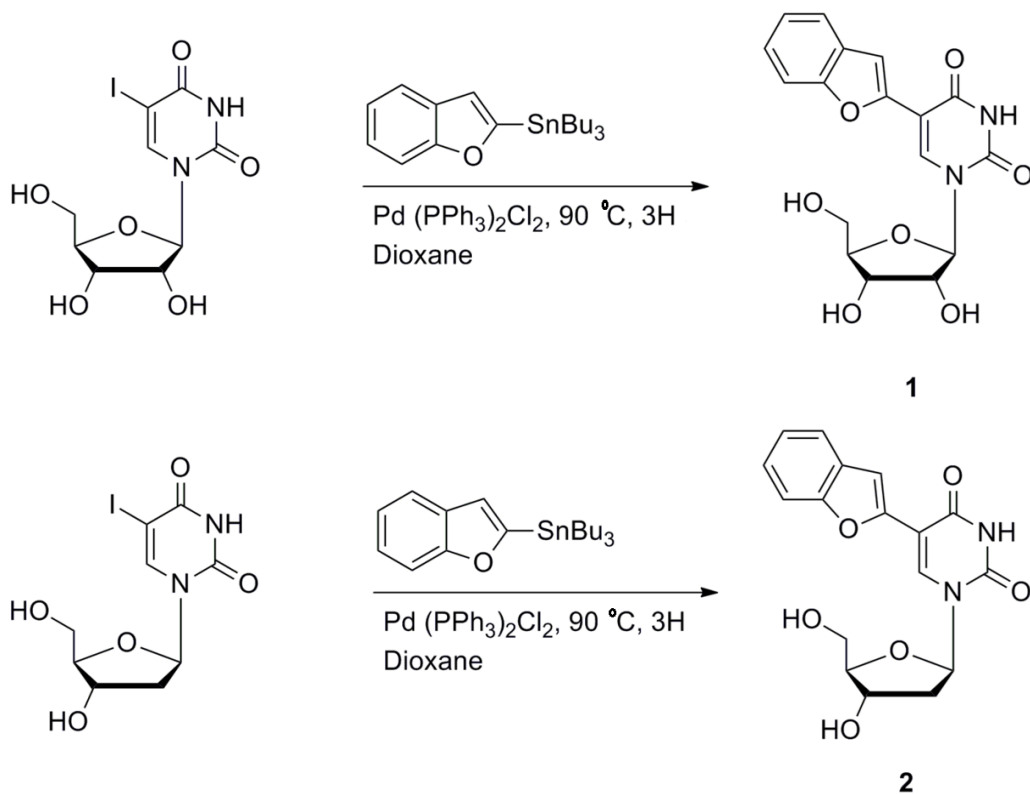
Scheme 1. Synthesis of modified ribonucleoside **1** (BFU) and deoxyribonucleoside **2** (BFdU).[45,47]

3.2. Fluorescent properties of BFdU in Anionic Micelles

When sodium dodecyl sulphate, where the head group is a sulphate group and the hydrophobic tail consists of 12 C long alkyl chain, is added into a polar solvent like water, after the critical micellar concentration, the SDS molecules start self-assembling into spherical structures where the anionic sulphate groups are oriented to the outside and the inner core consists of hydrophobic alkyl chains. After the formation of micelles, the viscosity increases and there is a drastic decrease in the surface tension. The fluorescent nucleoside analogue BFdU has been shown to be environment sensitive and shows an excellent solvatochromism. The fluorescent nucleoside analogue, shows an enhancement in the fluorescence intensity in viscous medium and a hypsochromic shift with decrease in the solvent polarity.[45]

So, to check the ability of this molecule to sense the changes in the physical properties before and after CMC, and possibly be able to determine the CMC, various fluorescence studies of BFdU (5 µM) in SDS of different concentrations have been performed. Figure 5 depicts the steady-state fluorescence spectrum of BFdU in aqueous solutions of SDS at various concentrations. The emission spectra of BFdU at very low concentrations of SDS is very similar to that of water and this is true for the first few concentrations where there are no appreciable changes in either the emission intensity or the emission maximum. But with an increase in the SDS concentration, there is an enhancement in the fluorescence intensity, which gets saturated at higher concentrations of SDS. There is also a hypsochromic shift (from 448 nm to 435 nm) in the emission maximum with the increase in the SDS concentration. Further to estimate the CMC of SDS, plot of fluorescence intensity (at 448 nm) versus concentration of SDS was fitted with a non-linear sigmoidal curve fitting using Boltzmann function (Figure 6). The center of the sigmoid which corresponds to the CMC was found to be 10.1 ± 0.3 mM which is in good agreement with the literature CMC values of SDS (8.0–8.5 mM).[32,48]

The enhancement in the fluorescence intensity (2-fold) and a blue shift of 13 nm indicate that at very low SDS concentrations (much below its CMC value), BFdU is present in an environment which is highly polar and has very low viscosity like that of water. Also with an increase in the SDS concentration (above CMC), the fluorescence

spectrum gets blue shifted which indicates that the environment around BFdU is getting more non-polar. At SDS concentrations above the CMC BFdU is solubilized in a relatively less polar environment with an emission maximum of 436 nm at 12 mM SDS.
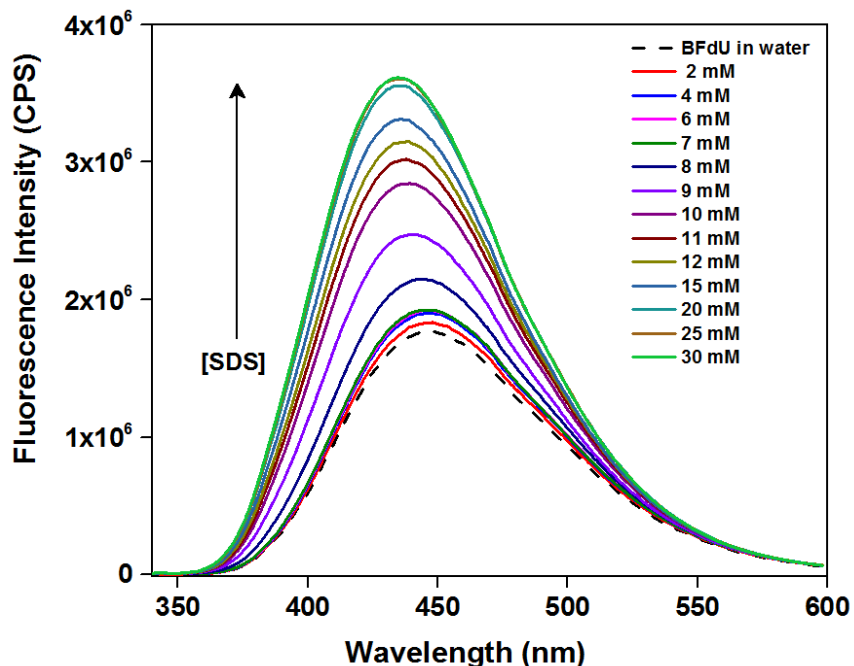
Figure 5. Emission spectra of BFdU (5 µM) in various concentrations of SDS solutions (aqueous). The samples were excited at 322 nm. The excitation and emission slit widths were kept at 2 and 3 nm, respectively.
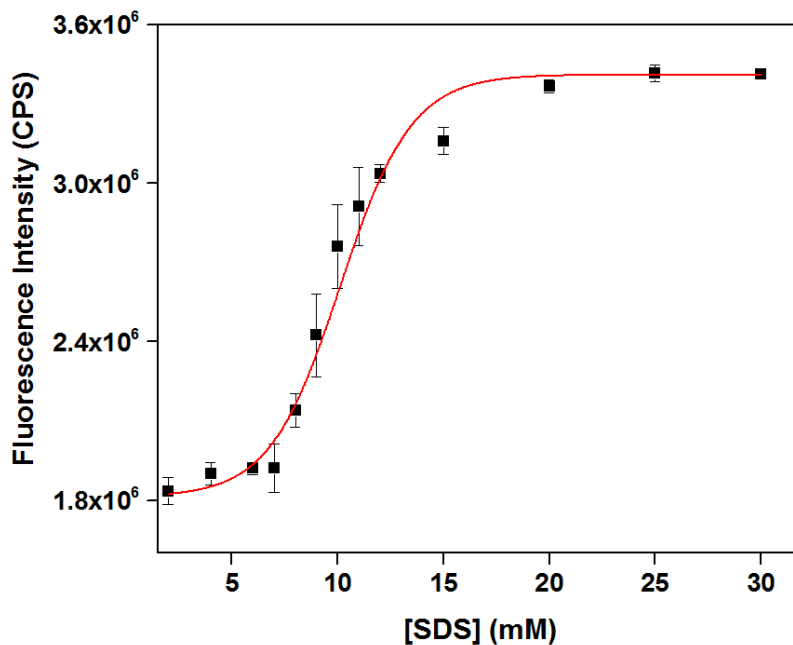
Figure 6. Plot of fluorescence intensity of BFdU at 448 nm as a function of SDS concentration.

The fluorescence anisotropy studies of BFdU carried out at three different conditions, one below the CMC value of SDS (where there are no micelles) i.e. at 2 mM, one around CMC value (where the micelles start forming) i.e. at 10 mM and one above CMC value (where the majority of the molecules are in micellar state), indicate that there is an increase in the anisotropy value with increase in SDS concentration (Table 1). This implies that there is an increase in viscosity with increase in SDS concentration. It appears that the nucleoside analogue gets stuck in between the micellar structures. The enhancement in the fluorescence intensity (up to two fold) with the increase in the SDS concentration is governed by two factors which seem to be in competition here. As reported by Tanpure et al.,[45] fluorescence intensity of BFdU gets quenched with the decrease in the solvent polarity and shows an enhancement in the fluorescence intensity with an increase in the viscosity of the solvent. This implies that when the environment around BFdU gets more non-polar, its fluorescence intensity should get quenched however here it is getting enhanced which indicates that viscosity is over riding the effect of solvent polarity.

Table 1. Excited-state lifetime and fluorescence anisotropy of the ribonucleoside BFdU (5 µM) in SDS.

Sample	τ_{av} (ns)[a]	r[a]
BFdU in water	2.20	0.017
2 mM SDS	1.27	0.017
10 mM SDS	1.58	0.030
20 mM SDS	1.79	0.037

[a]Standard deviations for the average life time (τ_{av}) and anisotropy (r) are ≤0.02 ns and 0.002, respectively.

Excited-state kinetics study indicates that with increase in SDS concentration the lifetime of BFdU increases and is highest in water (Figure 7, Table 1). Earlier reports by Tanpure et al. show that the life time of BFdU is maximum in water and decreases with decrease in polarity of the solvent.[45] This also further supports the blue shift in the

emission maximum with increase in SDS concentration confirming that the environment around BFdU below and above CMC is different.
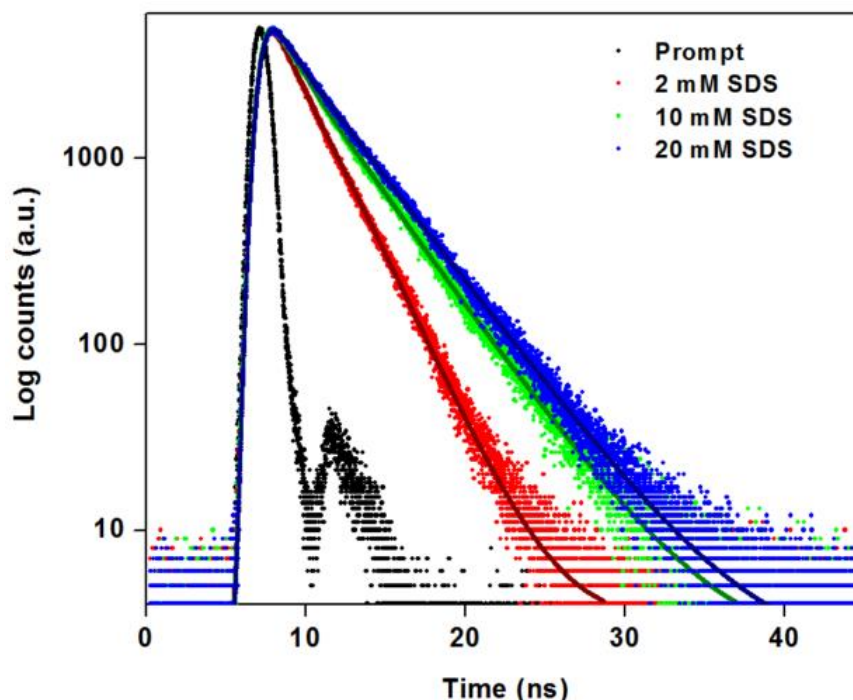
Figure 7. Excited-state decay profile of BFdU in different concentrations of SDS. Here the decay profile of laser is shown in black (prompt). Curve fits are in solid lines.

Based on the above observations it can be concluded that, below CMC, BFdU is present in a polar environment but in a less viscous medium. This results in high rate of rotation along the single bond connecting the benzofuran to uridine. So the effective conjugation is reduced, which is evident with the low fluorescence intensity and the emission maximum. When there are micelles formed, BFdU gets rigidified in the micellar structures at the interface of micellar heads and the hydrophobic tails, which is relatively less polar. It seems that the benzofuran part of BFdU is embedded in the hydrophobic chain of SDS and the hydrophilic sugar part at micellar head groups (Figure 8), which is evident with the higher anisotropy values, increase in fluorescence intensity and a blue shifted emission maximum.
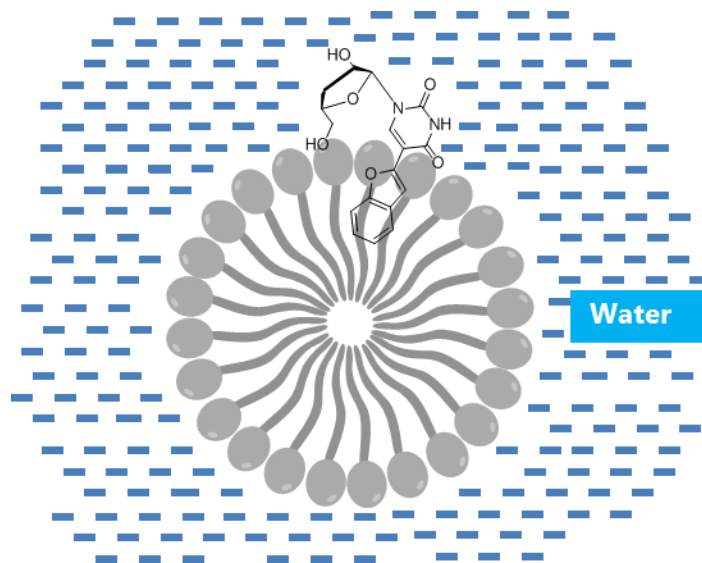
Figure 8. Diagram depicting the entrapment of BFdU in the micellar aggregates of SDS. Not to scale.

3.3. Fluorescence properties of BFU in AOT reverse micelles

BFdU successfully senses the microenvironment in the micelles and the changes in the physical properties like viscosity and polarity. This prompted its use as a probe in studying the microenvironment of reverse micellar structures. The inner water core of AOT reverse micelles has been shown to be very different than the bulk water and is very similar to the environment present at the interfaces of the membranes.[49] Thus, they act as cell mimicking systems providing macromolecular crowding effect. The properties of the inner water core changes with the amount of water present in the core which is given by W_0 value.[40]

Since the microenvironment inside the reverse micelles is quite different depending on the W_0 value, steady-state fluorescence and lifetime measurements of the fluorescent nucleoside analogue BFdU were performed. However, there were solubility issues with BFdU in water. Even when the final concentration of the deoxy uridine nucleoside analogue was set to 1 μM from 5 μM, BFdU had solubility issues. In order to solve this issue monophosphorylation of BFdU and BFU (ribose version of BFdU) has been done. This would increase the hydrophilicity of the molecules drastically. These monophosphates can be used to study the ionic-ionic interactions

between the fluorophores and the AOT reverse micelles. These studies will be performed subsequently.

BFU has an extra –OH group as compared to BFdU, which increases its solubility in water. Also the photophysical properties of BFdU and BFU are very similar. Both have the excitation maximum at 322 nm and show solvatochromism. So taking all these things into account fluorescence steady state and life time studies of BFU have been done in AOT reverse micelles with different W_0 values. Steady-state fluorescence studies show that at the lowest W_0 value (i.e. 0.7) BFU shows an emission spectrum which has very high fluorescence intensity and is blue shifted (λ_{em} = 405 nm, Figure 9). With increase in the W_0 values, the spectrum shows that there is a fluorescence quenching and also a red shift in emission maximum. The emission spectra show drastic quenching in the emission till the W_0 value of 5.6 which on further rise start saturating. On the other hand, there is a continuous red shift in the emission maximum with increase in W_0 value. One other important and interesting point is that the emission maximum at W_0 = ~11 (λ_{em} = 423 nm) is very similar to the emission maximum of BFU in methanol.[47] Similar studies done by Hazra et al. and Belletête have shown that the environment in the inner core of AOT reverse micelles resembles the environment of methanol.[50,51]

Fluorescence anisotropy studies revealed that, as the W_0 value increases the anisotropy decreases (Table 2). This implies that the viscosity of the water core is dependent on the W_0 value. At lower water concentration the water is more viscous and as the W_0 is increased the viscosity decreases. Earlier studies have also reported that the motion of water is greatly reduced when it is encapsulated in the inner core of the AOT reverse micelles[36,37]
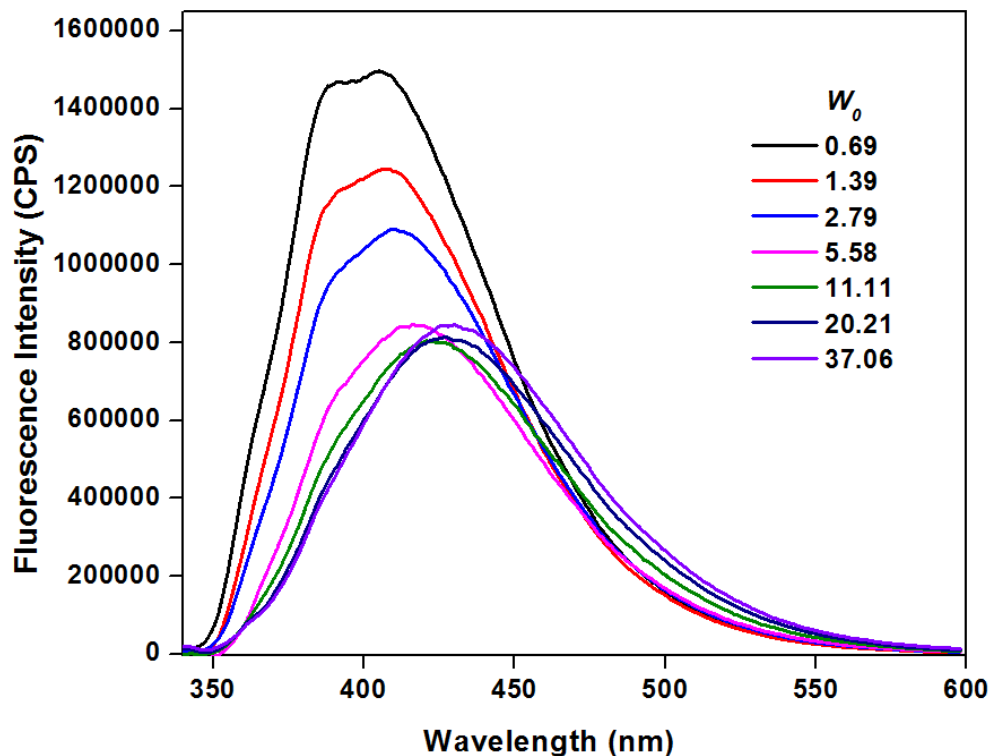
Figure 9. Emission spectra of ribonucleoside BFU (1 µM) in AOT reverse micelles as a function of W_0. Samples were excited at 322 nm. Excitation and emission slit widths were kept at 3 and 4 nm, respectively.

Table 2. Fluorescence Anisotropy of the ribonucleoside, BFU (1 µM) in AOT reverse micelles at different W_0 values.

W_0	$r^{[a]}$
0.7	nd
1.4	0.137
2.8	0.144
5.6	0.126
11.1	0.095
20.2	0.074
37.1	0.058

[a]Standard deviation for anisotropy (r) is 0.002. nd = not determined.

Based on the trend seen in the fluorescence steady-state experiments, it can be concluded that when the W_0 value is very low the ribonucleoside analogue, BFU, is incorporated in the reverse micellar heads where the molecule is getting rigidified. Because of this the rotation of aryl-aryl single bond is restricted, resulting in an intense fluorescence signal. This is because, at lower W_0 values most of the water molecules are interacting with the hydrophilic head groups and the viscosity of this aqueous layer in the core of reverse micelles is high.[10] As the W_0 is increased, around a W_0 value of 11, there are enough water molecules to form well-structured domain which is less viscous and relatively more polar. This results is a quenched fluorescence signal and a red shifted emission maximum. It can be predicted that at this W_0 Value the ribonucleoside analogue shifts its position from the interface to the inner core where there is a well-defined water pool. Also when the water content is further increased, there is no significant change in the fluorescence intensity which indicates that after this W_0 value the change in the viscosity is gradual. This is also supported by the trend in the fluorescence anisotropy values. The change in the emission maxima to the red region implies that the environment inside the reverse micelles gets more polar on addition of water but is still very different than the bulk water. Similar results have been reported by Maroti et al.[34]

3.4. Fluorescent modification of human telomeric DNA repeat (BFGQ)

G-quadruplexes are a class of nucleic acid secondary structures formed by stacking of guanine rich regions. They show a diverse conformational change and stability. This change depends on various factors like the bases present in the loops, the environment, the stabilising metal ions and other solvent properties like hydration effects, macromolecular crowding effects etc.[13–15] G-quadruplexes fold into anti-parallel structures in the presence of sodium ions and into a mixed-hybrid conformation when potassium ions are present. They form extensively parallel conformations in poly ethylene glycol medium, which has been widely used as a macromolecular crowding agent.[12,15–17] They are present in telomeres and at the transcription promoter regions.[21,22] They are involved in a lot of biological process like gene regulation, maintenance of chromosome stability and gene silencing. These structures are directly

involved in a lot of cancers, thus, making them very important targets for cancer therapy.[15,22–24,52,53] So, their study is of great biological importance. But, so far all the tools that have been used to study their conformational dynamics, have made use of antibody labelling or fluorescent dyes, which selectively go and bind to G-quadruplex structures.[15,19,20,26,27,54–57] However, in all these cases, the molecules used to probe are big and might have an effect on the stability.[12] Development of non-perturbing probes in order to study the conformational changes in the G-quadruplexes is highly desired.

Based on the photophysical studies of BFdU in micellar and BFU in reverse micellar systems, it can be concluded that nucleoside analogue can sense the changes in the microenvironment of the micelles and in the core of reverse micelles and hence is an efficient environment sensitive probe. This encouraged the incorporation of BFdU in a 22-mer human telomeric DNA repeating sequence (BFGQ) which is known to form G-quadruplex structures.

The fluorescent nucleoside analogue was incorporated at the 11th position from the 5' end. This would place the nucleoside analogue in the first position of the diagonal loop in an anti-parallel structure. However, if the BFGQ folds into a hybrid structure, which generally happens in the presence of K$^+$ ions in aqueous medium, BFdU is the first molecule in the propeller loop. The incorporation was done under standard solid-phase oligonucleotide synthesis conditions by one of my laboratory colleagues, Arun Tanpure. Later purification was done by PAGE under denaturing conditions. The quantification was done in UV-visible spectroscopy by Arun Tanpure. After quantification the concentration of the BFGQ sequence was found to be 723 µM.
The sequence of fluorescent BFGQ used in this study:

<div align="center">5' d(AGG GTT AGG G2T AGG GTT AGG G) 3'</div>

3.5. Photophysical studies of BFGQ in different ionic conditions

In aqueous buffer: To check the ability to sense metal ion dependent conformational changes in the telomeric sequence, fluorescence steady-state and lifetime studies of BFdU labelled oligonucleotide sequence BFGQ were done in Tris buffer with 50 mM of Na$^+$ or K$^+$ ions. BFGQ in tris buffer containing 50 mM KCl displayed an intense emission

band around 440 nm, which was nearly 15-fold higher than the corresponding duplex (Figure 10). Interestingly, in Tris buffer containing 50 mM NaCl BFGQ exibited remarkable enhancemnt in fluoresence intensity (~40-fold) as compared to corresponding duplex. Previous results show that the G-quadruplex forming sequences fold into different conformations depending on the stabilising metal ions: antiparallel in the presence of Na^+ ions and hybrid structures in the presence of K^+ ions.[12] BFdU can clearly distinguish between the antiparallel G-quadruplex conformations in the presence of Na^+ ions and the hybrid-type conformations in K^+ ions. These observations were found to be in good agreement with the results obtained by one of my lab colleagues earlier (unpublished data).
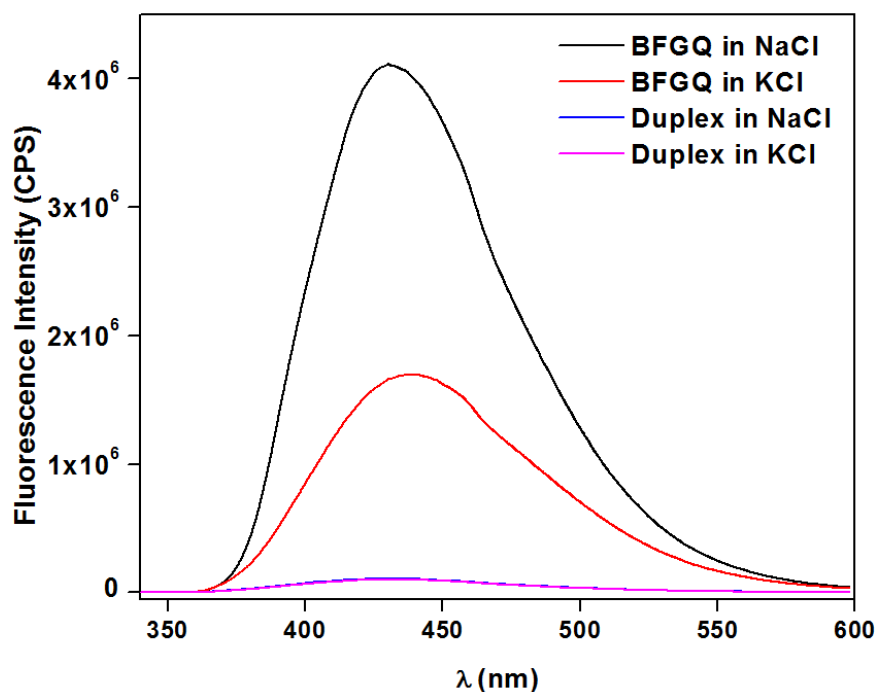
Figure 10. Steady-state fluorescence spectra of BFGQ (4 µM) and the duplexes (4 µM) in Tris buffer (10 mM, 7.5 pH) with Na^+ or K^+ (50 mM). The oligonucleotides were excited at 322 nm. The excitation and emission slit widths were kept at 2 and 4 nm, respectively.

In AOT reverse micelles: The use of BFdU in cell based systems is restricted due to its excitation maximum in the UV region.[47] But AOT reverse micelles, act as cell mimicking systems to carry out the cell based studies and are UV transparent. There are reports where people have used AOT reverse micelles as cell mimicking agents to study the

structure based studies of oligonucleotides.[34,58,59] So, studies of cation dependent conformational changes of GQs in a cell-like medium using AOT (sodium salt) reverse micelles were done. All the studies were performed at W_0 value of 20.

BFGQ in reverse micelles displayed nearly 40-fold enhancement in fluoresence intensity as compared to corresponding duplex in Na^+ (Figure 11). Interestingly, BFGQ in the presence of K^+ ions also exhibited similar enhancement in fluorescence intensity. This suggests that in the inner water core of AOT reverse micelles the oligonucleotide forms antiparallel G-quadruplex conformation irrespective of the stabilising metal ion.
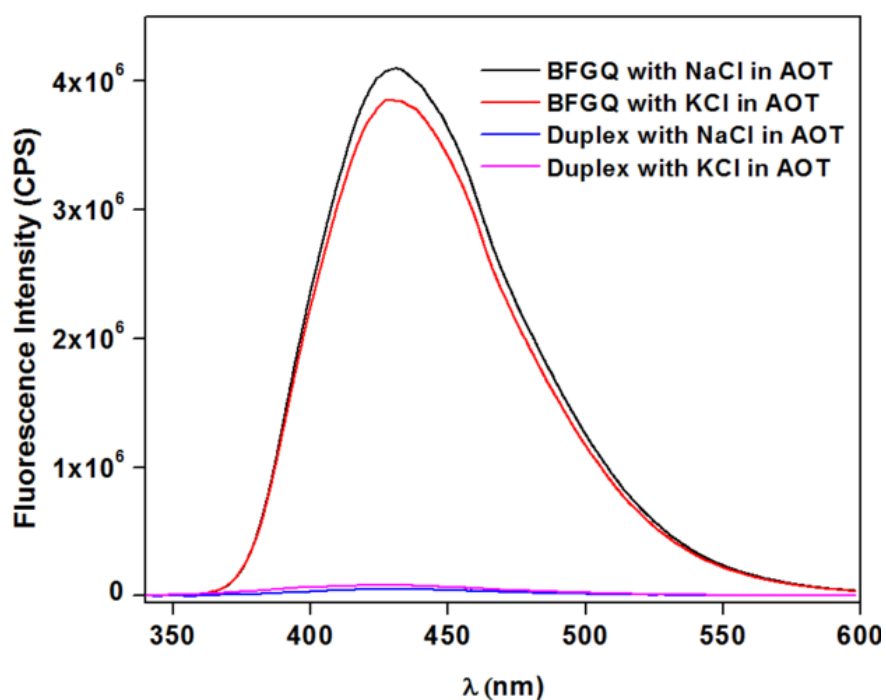
Figure 11. Steady state fluorescence spectra of BFGQ(4 µM) and the duplexes(4 µM) in AOT reverse micelles ($W_0 = 20$) with Na^+ or K^+ (50 mM). The oligonucleotides were excited at 322 nm. The excitation and emission slit widths were kept at 2 and 4 nm, respectively.

There is restricted motion in the inner core of reverse micelles and the environment is viscous compared to bulk water. So the expected result was that, in AOT reverse micelles, there would be an enhancement in the fluorescence intensity of the BFGQ as compared to buffer system. However, from the bar diagram it is evident that the emisssion intensity of G-quadruplex in aqueous buffer containing Na^+ ions and in

the AOT reverse micelles (containing sodium and potassium ions) are very similar (Figure 12). This observation suggests that BFGQ in AOT (sodium salt) reverse micelles adopts an antiparallel structure irrespective of the added Na^+ or K^+ ions. These results are in consensus with earlier reports.[59,60] Taken together, these results imply that the benzofuran modified uridine, when incorporated into GQ forming structures, successfully senses the metal ion-dependent changes in the conformation in AOT reverse micelles.
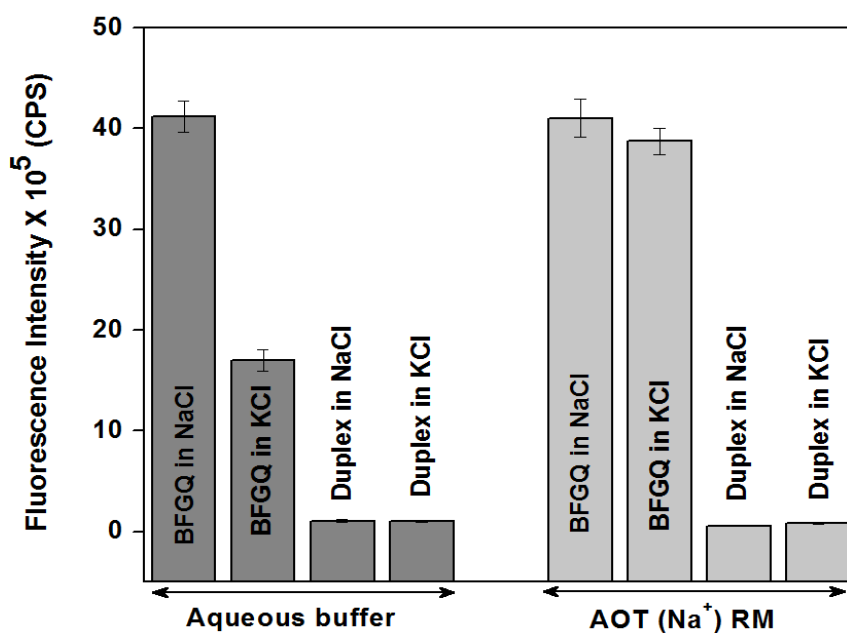
Figure 12. Fluorescence intensity of BFGQ (1 µM) in aqueous buffer and in AOT reverse micelles at the respective emission maximum. Samples were excited at 322 nm. The excitation and emission slit widths were kept at 2 and 4, respectively.

3.6. Circular dichroism studies

To confirm that the structures formed are indeed G quadruplexes, CD studies were performed. GQ forming human telomeric sequence in 10 mM Tris (7.5 pH) has the following characteristic peaks:

- In the presence of Na^+ : a positive peak at ~290 nm and a negative peak at ~260 nm indicates the formation of antiparallel G-quadruplex structures.

- In the presence of K^+ : a positive peak at ~290 nm and a positive shoulder at ~270 nm, indicates the formation hybrid-type structure.[12]

CD analysis of BFGQ sequences in buffer containing 50 mM NaCl shows a positive peak at 295 nm and a negative peak at 263 nm confirming that in buffers containing NaCl salts BFGQ fold into antiparallel conformations (Figure 13). In buffer containing 50 mM KCl, there is a positive peak at 292 nm and a shoulder peak at 275 nm. This shows that the structures formed are of hybrid-type (Figure 13, Table 3). When encapsulated in AOT reverse micelles, BFGQ in 50 mM of both Na^+ and K^+ show positive peaks at 295 and 296 nm, respectively, and a negative peak at 263 nm. This implies that BFGQ are folded into antiparallel GQ structures irrespective of ionic conditions (Figure 14, Table 3).
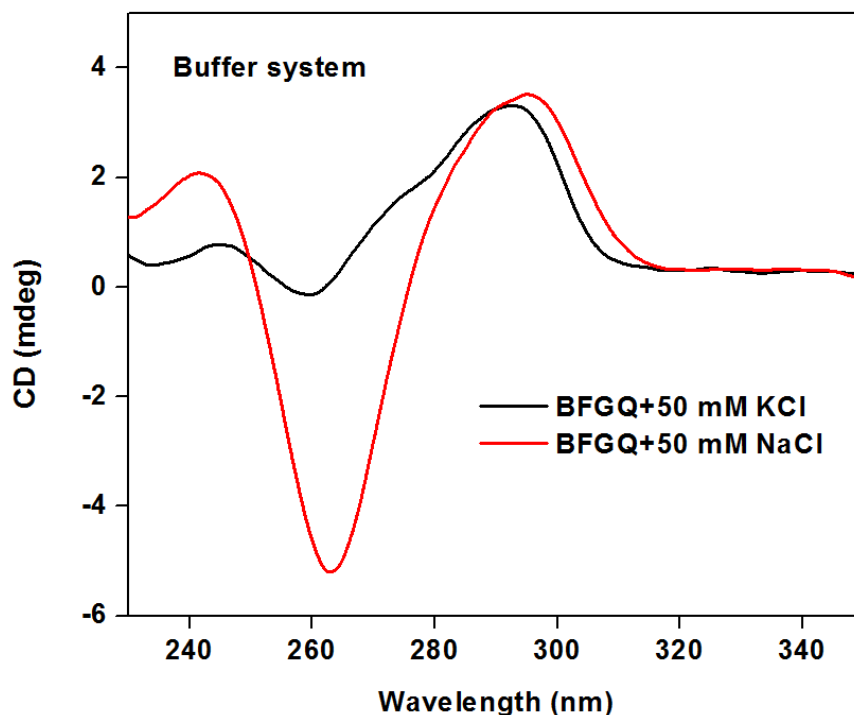
Figure 13. CD spectra of BFGQ (4 µM) in buffers containing Na^+ or K^+ ions (50 mM).

Table 3. Ellipticity and the position of peaks for the BFGQ G-quadruplexes in buffers and AOT RM containing Na^+ or K^+ ions.

Samples	+ve peak		-ve Peak	
	Peak position (nm)	Ellipticity (mdeg)	Peak position(nm)	Ellipticity (mdeg)
BFGQ in NaCl	295	3.520	263	-5.199
BFGQ in KCl	292	3.310	A positive shoulder peak around 275 nm	
$W_0=20$, BFGQ in NaCl	295	4.850	263	-6.098
$W_0=20$, BFGQ in KCl	296	4.240	263	-6.043
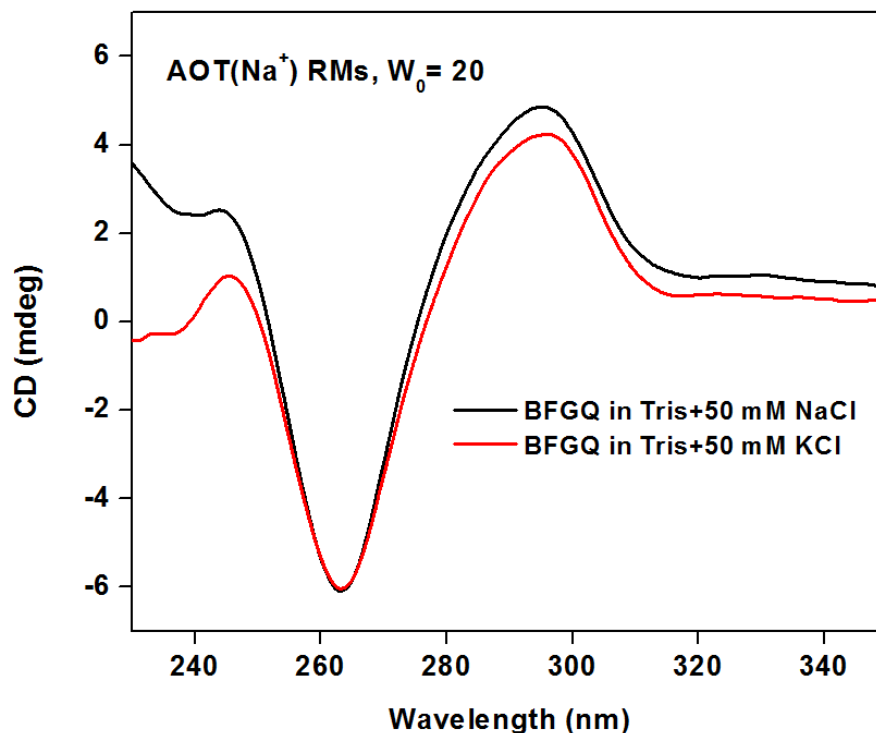
Figure 14. CD spectra of BFGQ (4 µM) in AOT reverse micelles ($W_0 = 20$) containing Na^+ or K^+ ions (50 mM).

Human telomeric repeat in aqueous buffer containing Na^+ and K^+ is known to form antiparallel and mixed-type GQ structures, respectively. In AOT reverse micelles, however even in the presence of 50 mM KCl BFGQ folds into antiparallel structure. This supports the fluorescence data that BFdU when incorporated into a GQ sequence, can sense the metal ion-dependent conformational changes in AOT reverse micellar systems. The CD studies in buffers and AOT reverse micelles follow the similar trend shown by Li, Sugimoto and Ho groups.[59–61] The AOT surfactant used for the experiments has Na^+ as the counter ion. So, when water is encapsulated in the inner core, at very low W_0 values these Na^+ ions and the water molecules are interacting with the ionic head groups. But as the water content is increased even though most of the Na^+ ions reside in the Stern layer, some of them are dissociated in the inner water pool. So, even when K^+ is added externally, BFGQ must be forming antiparallel conformation simply because of the presence of these dissociated Na^+ ions. Also compared to Na^+ and K^+, G-quadruplexes are known to preferentially bind to K^+ ions. But the antiparallel nature of the GQ structures suggests that this can be possible only if the concentration of Na^+ ions is very high compared to K^+ ions. Indeed in this study we have used 200 mM AOT (sodium salt). These results are in agreement with the previous results.[59,60] Furthermore, the enhancement in fluorescence intensity exhibited by BFGQ as compared to corresponding duplex in AOT is likely due to the following reasons–rigidification of the fluorophore and or reduced electron transfer and stacking interaction with neighboring bases.[62]

4. Conclusions

The present work focuses on the use of an environment-sensitive fluorescent nucleoside analogue based on a 5-(benzofuran-2-yl)pyrimidine core to study the structure of a biologically important oligonucleotide sequence which is found in human telomeres and folds into G-quadruplex structures. Photophysical studies show that the nucleoside analogue positively senses the changes in the physical properties like viscosity and polarity in micelles and in the inner aqueous core of reverse micelles. The sensitivity of the nucleoside was further utilized in studying the formation of G-quadruplex structures of human telomeric DNA repeats in reverse micelles. Our results clearly indicate that the fluorescent nucleoside analogue incorporated into human telomeric DNA reports the formation of G-quadruplex structure with significant enhancement in fluorescence intensity. The topology adopted by the telomeric DNA in confined environment was found to be antiparallel irrespective of the ionic conditions, which was also consistent with CD analysis. Taken together, these studies underscore the potential of benzofuran-modified nucleoside analogue as an effective probe for DNA G-quadruplex in cell-like confined environment.

5. References

1. Murat, P. & Balasubramanian, S. Existence and consequences of G-quadruplex structures in DNA. *Curr. Opin. Genet. Dev.* **25,** 22–29 (2014).

2. Korostelev, A., Trakhanov, S., Laurberg, M. & Noller, H. F. Crystal structure of a 70S ribosome-tRNA complex reveals functional interactions and rearrangements. *Cell* **126,** 1065–1077 (2006).

3. Bardaro, M. F. & Varani, G. Examining the relationship between RNA function and motion using nuclear magnetic resonance. *Wiley Interdiscip. Rev. RNA* **3,** 122–132 (2012).

4. Nguyen, P. & Qin, P. Z. RNA dynamics: perspectives from spin labels. *Wiley Interdiscip. Rev. RNA* **3,** 62–72 (2012).

5. Phelps, K., Morris, A. & Beal, P. Novel modifications in RNA. *ACS Chem. Biol.* **7,** 100–109 (2011).

6. Srivatsan, S. G. & Sawant, A. a. Fluorescent ribonucleoside analogues as probes for investigating RNA structure and function. *Pure Appl. Chem.* **83,** 213–232 (2010).

7. Wilson, J. N. & Kool, E. T. Fluorescent DNA base replacements: Reporters and sensors for biological systems. *Org. Biomol. Chem.* **4,** 4265–4274 (2006).

8. Ranasinghe, R. T. & Brown, T. Fluorescence based strategies for genetic analysis. *Chem. Commun.* **124,** 5487–5502 (2005).

9. Marttila, C. M. Structures for Polyinosinic Acid and Polyguanylic Acid. *Biochem. J.* **141,** 537–543 (1974).

10. Hasegawa, M. & Sugimura, T. Microviscosity in water pool of Aerosol-OT reversed micelle determined with viscosity-sensitive fluorescence probe, auramine O, and fluorescence depolarization of. *J. Phys. Chem.* **98,** 2120–2124 (1994).

11. Sen, D. & Gilbert, W. Formation of parallel four-stranded complexes by guanine-rich motifs in DNA and its implications for meiosis. *Nature* **334,** 364–366 (1988).

12. Bhasikuttan, A. C. & Mohanty, J. ChemComm Targeting G-quadruplex structures with extrinsic fluorogenic dyes : promising fluorescence sensors. *Chem. Commun.* (2015).

13. Sattin, G., Artese, A., Nadai, M. & Costa, G. Conformation and stability of intramolecular telomeric g-quadruplexes: Sequence effects in the loops. *PLoS One* **8,** 1–16 (2013).

14. Luigi Petraccone, Anna Malafronte, Jussara Amato, C. G. G-Quadruplexes from Human Telomeric DNA: How Many Conformations in PEG Containing Solutions? *J. Phys. Chem. B* **116,** 2294–2305 (2012).

15. Hong, Y. *et al.* Label-Free Fluorescent Probing of G-Quadruplex Formation and Real-Time Monitoring of DNA Folding by a Quaternized Tetraphenylethene Salt with Aggregation-Induced Emission Characteristics. *Chem. - A Eur. J.* **14,** 6428–6437 (2008).

16. Xue, Y., Kan, Z., Wang, Q. & Yao, Y. Human telomeric DNA forms parallel-stranded intramolecular G-quadruplex in K+ solution under molecular crowding condition. *J. Am. Chem. Soc.* **129,** 11185–11191 (2007).

17. Buscaglia, R. *et al.* Polyethylene glycol binding alters human telomere G-quadruplex structure by conformational selection. *Nucleic Acids Res.* **41,** 7934–7946 (2013).

18. Sharma, V. R. & Sheardy, R. D. The human telomere sequence, (TTAGGG)4, in the absence and presence of cosolutes: a spectroscopic investigation. *Molecules* **19,** 595–608 (2013).

19. Biffi, G., Tannahill, D., McCafferty, J. & Balasubramanian, S. Quantitative visualization of DNA G-quadruplex structures in human cells. *Nat. Chem.* **5,** 182–186 (2013).

20. Biffi, G., Di Antonio, M., Tannahill, D. & Balasubramanian, S. Visualization and selective chemical targeting of RNA G-quadruplex structures in the cytoplasm of human cells. *Nat. Chem.* **6,** 75–80 (2014).

21. Yuan, L. *et al.* Existence of G-quadruplex structures in promoter region of oncogenes confirmed by G-quadruplex DNA cross-linking strategy. *Sci. Rep.* **3,** 1811 (2013).

22. Balasubramanian, S. & Neidle, S. G-quadruplex nucleic acids as therapeutic targets. *Curr. Opin. Chem. Biol.* **13,** 345–353 (2009).

23. Bugaut, A. & Balasubramanian, S. 5'-UTR RNA G-quadruplexes: translation regulation and targeting. *Nucleic Acids Res.* **40,** 1–15 (2012).

24. Shalaby, T. *et al.* G-Quadruplexes as Potential Therapeutic Targets for Embryonal Tumors. *Molecules* **18,** 12500–12537 (2013).

25. Murat, P. *et al.* G-quadruplexes regulate Epstein-Barr virus-encoded nuclear antigen 1 mRNA translation. *Nat. Chem. Biol.* **10,** 358–364 (2014).

26. Luedtke, N. W. Targeting G-Quadruplex DNA with Small Molecules. *Chim. Int. J. Chem.* **63,** 134–139 (2009).

27. Di Antonio, M. *et al.* Selective RNA Versus DNA G-Quadruplex Targeting by In Situ Click Chemistry. *Angew. Chemie Int. Ed.* **51,** 11073–11078 (2012).

28. Johnson, J., Okyere, R., Joseph, A., Musier-forsyth, K. & Kankia, B. Quadruplex formation as a molecular switch to turn on intrinsically fluorescent nucleotide analogs. *Nucleic Acids Res.* **41,** 220–228 (2013).

29. JoonáLee, I., WuáYi, J. & HyeanáKim, B. Probing the stable G-quadruplex transition using quencher-free end-stacking ethynyl pyrene–adenosine. *Chem. Commun.* 2817–2819 (2007).

30. Dumas, A. & Luedtke, N. W. Cation-Mediated Energy Transfer in G-Quadruplexes Revealed by an Internal. *J. Am. Chem. Soc.* **132,** 18004–18007 (2010).

31. Tanhaei, B. *et al.* Experimental Study of CMC Evaluation in Single and Mixed Surfactant Systems, Using the UV–Vis Spectroscopic Method. *J. Surfactants Deterg.* **16,** 357–362 (2012).

32. Bahri, M. a. *et al.* Investigation of SDS, DTAB and CTAB micelle microviscosities by electron spin resonance. *Colloids Surfaces A Physicochem. Eng. Asp.* **290,** 206–212 (2006).

33. Mitra, R. K., Sinha, S. S. & Pal, S. K. Interactions of Nile Blue with Micelles, Reverse Micelles and a Genomic DNA. *J. Fluoresc.* **18,** 423–432 (2007).

34. Pawar, M. G. & Srivatsan, S. G. Environment-Responsive Fluorescent Nucleoside Analogue Probe for Studying Oligonucleotide Dynamics in a Model Cell-like Compartment. *J. Phys. Chem. B* **117,** 14273–14282 (2013).

35. Martinez, A. & Dominguez, L. Probing the structure and dynamics of confined water in AOT reverse micelles. *J. Phys. Chem. B* **117,** 7345–7351 (2013).

36. Riter, R. E., Willard, D. M. & Levinger, N. E. Water Immobilization at Surfactant Interfaces in Reverse Micelles. *J. Phys. Chem. B* **5647,** 2705–2714 (1998).

37. Amico, P., Onori, G. & Santucci, A. Infrared Absorption and Water Structure in Aerosol OT Reverse Micelles . *NUOVO Cim.* **17,** 1053–1065 (1995).

38. Hirose, Y., Yui, H. & Sawada, T. The Ultrafast Relaxation Dynamics of a Viscosity Probe Molecule in an AOT-Reversed Micelle : Contribution of the Specific

Interactions with the Local Environment. *J. Phys. Chem. B* **108,** 9070–9076 (2004).

39.   Zhang, X., Jackson, J. K. & Burt, H. M. Determination of surfactant critical micelle concentration by a novel fluorescence depolarization technique. *J. Biochem. Biophys. Methods* **31,** 145–150 (1995).

40.   Bru, R., Sanchez-ferrer, A. & Garcia-carmona, F. Kinetic models in reverse micelles. *Biochem. J.* **739,** 721–739 (1995).

41.   Kitchens, C. L., Bossev, D. P. & Roberts, C. B. Solvent Effects on AOT Reverse Micelles in Liquid and Compressed Alkanes Investigated by Neutron Spin - Echo Spectroscopy. *J. Phys. Chem. B* **110,** 20392–20400 (2006).

42.   Karukstis, K. & Frazier, A. Characterization of the microenvironments in AOT reverse micelles using multidimensional spectral analysis. *J. Phys. Chem.* **3654,** 11133–11138 (1996).

43.   Gochman-hecht, H. & Bianco-peled, H. Structure of AOT reverse micelles under shear. *J. Colloid Interface Sci.* **288,** 230–237 (2005).

44.   Costa, S. Probing the interface polarity of AOT reversed micelles using centrosymmetrical squaraine molecules. *Phys. Chem. Chem. Phys.* **1,** 4409–4416 (1999).

45.   Tanpure, A. a & Srivatsan, S. G. Synthesis and photophysical characterisation of a fluorescent nucleoside analogue that signals the presence of an abasic site in RNA. *Chembiochem* **13,** 2392–2399 (2012).

46.   Horn, W. Van, Ogilvie, M. & Flynn, P. Reverse micelle encapsulation as a model for intracellular crowding. *J. Am. Chem. Soc.* **131,** 8030–8039 (2009).

47.   Tanpure, A. A. & Srivatsan, S. G. A Microenvironment-Sensitive Fluorescent Pyrimidine Ribonucleoside Analogue: Synthesis, Enzymatic Incorporation, and Fluorescence Detection of a DNA Abasic Site. *Chem. Eur. J.* **17,** 12820–12827 (2011).

48.   Mohr, A. *et al.* A New Pyrene-Based Fluorescent Probe for the Determination of Critical Micelle Concentrations. *J. Phys. Chem. B* **111,** 12985–12992 (2007).

49.   Fioretto, D. *et al.* Infrared and Dielectric Study of Ca (AOT) 2 Reverse Micelles. *J. Phys. Chem. B* **103,** 2631–2635 (1999).

50.   Belletste, M., Lachapelle, M. & Durocher, G. Polarity of AOT Micellar Interfaces: Use of the Preferential Solvation Concepts in the Evaluation of the Effective Dielectric Constants. *J. Phys. Chem.* **94,** 5337–5341 (1990).

51. Hazra, P. & Sarkar, N. Intramolecular charge transfer processes and solvation dynamics of coumarin 490 in reverse micelles. *Chem. Phys. Lett.* **342,** 303–311 (2001).

52. Collie, G. W. & Parkinson, G. N. The application of DNA and RNA G-quadruplexes to therapeutic medicines. *Chem. Soc. Rev.* **40,** 5867–5892 (2011).

53. Millevoi, S., Moine, H. & Vagner, S. G-quadruplexes in RNA biology. *Wiley Interdiscip. Rev. RNA* **3,** 495–507 (2012).

54. Garavís, M. & López-Méndez, B. Discovery of Selective Ligands for Telomeric RNA G-quadruplexes (TERRA) through 19F-NMR Based Fragment Screening. *ACS Chem. Biol.* **9,** 1559–1566 (2014).

55. Yaku, H., Murashima, T., Miyoshi, D. & Sugimoto, N. Specific Binding of Anionic Porphyrin and Phthalocyanine to the G-Quadruplex with a Variety of *in vitro* and *in vivo* Applications. *Molecules* **17,** 10586–10613 (2012).

56. Rodriguez, R. *et al.* Small-molecule-induced DNA damage identifies alternative DNA structures in human genes. *Nat. Chem. Biol.* **8,** 301–310 (2012).

57. Granotier, C. *et al.* Preferential binding of a G-quadruplex ligand to human chromosome ends. *Nucleic Acids Res.* **33,** 4182–4190 (2005).

58. Workman, H. & Flynn, P. Stabilization of RNA oligomers through reverse micelle encapsulation. *J. Am. Chem. Soc.* **131,** 3806–3807 (2009).

59. Zhou, J. *et al.* Formation and stabilization of G-quadruplex in nanosized water pools. *Chem. Commun.* **46,** 1700–1702 (2010).

60. Ho, M.-C. & Chang, C.-W. Cationic and anionic reverse micelles as the molecular crowding container for G-quadruplex structure. *RSC Adv.* **4,** 20531–20534 (2014).

61. Pramanik, S., Nagatoishi, S. & Sugimoto, N. DNA tetraplex structure formation from human telomeric repeat motif (TTAGGG):(CCCTAA) in nanocavity water pools of reverse micelles. *Chem. Commun.* **48,** 4815–4817 (2012).

62. Sinkeldam, R., Greco, N. & Tor, Y. Fluorescent analogs of biomolecular building blocks: design, properties, and applications. *Chem. Rev.* **110,** 2579–2619 (2010).